European Cells and Materials Vol. 36 2018 (pages 142-155) DOI: 10.22203/eCM.v036a11 ISSN 1473-2262

COBALT IONS STIMULATE A FIBROTIC RESPONSE THROUGH MATRIX REMODELLING, FIBROBLAST CONTRACTION AND RELEASE OF PRO-FIBROTIC SIGNALS FROM MACROPHAGES

J. Xu[1], A. Nyga[2], W. Li[1], X. Zhang[1], N. Gavara[1], M.M. Knight[1] and J.C. Shelton[1,*]

[1] Institute of Bioengineering, School of Engineering and Materials Science, Queen Mary University of London, London, UK
[2] Institute for Bioengineering of Catalonia, 08028, Barcelona, Spain

Abstract

Many studies report the adverse responses to metal-on-metal (MoM) hip prostheses, with tissues surrounding failed implants prostheses revealing abundant tissue necrosis and fibrosis. These local effects appear to be initiated by metal ions released from the prosthesis causing the secretion of inflammatory mediators. However, little is known about the effects of the metal ions on tissue remodelling and pseudotumor formation, which are also associated with the failure of MoM hip prostheses. The peri-prosthetic soft-tissue masses can lead to pain, swelling, limited range of joint movement and extensive tissue lesion. To elucidate this cellular response, a multidisciplinary approach using both two- and three-dimensional (2D and 3D) *in vitro* culture systems was employed to study the effects of Co^{2+} and Cr^{3+} on human fibroblast activation and mechanobiology.

Co^{2+} induced a fibrotic response, characterised by cytoskeletal remodelling and enhanced collagen matrix contraction. This was associated with increased cell stiffness and contractile forces, as measured by atomic force microscopy and traction force microscopy, respectively. These effects were triggered by the generation of reactive oxygen species (ROS). Moreover, this fibrotic response was enhanced in the presence of macrophages, which increased the prevalence of α-smooth muscle actin (α-SMA)-positive fibroblasts and collagen synthesis. Cr^{3+} did not show any significant effect on fibroblast activation.

Co^{2+} promoted matrix remodelling by fibroblasts that was further enhanced by macrophage signalling. Use of alternative implant materials or manipulation of this fibrotic response could provide an opportunity for enhancing the success of prostheses utilising CoCr alloys.

Keywords: Cobalt chromium, fibroblast, extracellular matrix, cell mechanics, reactive oxygen species, fibrosis.

***Address for correspondence**: J.C. Shelton, Institute of Bioengineering, School of Engineering and Materials Science, Queen Mary University of London, London, UK.
Email: j.shelton@qmul.ac.uk

Introduction

More than one million metal-on-metal (MoM) hip replacement prostheses made from cobalt chromium (CoCr) alloys are implanted worldwide to restore mobility and improve the quality of life in patients suffering from severe osteoarthritis or femoral fractures (Kwon *et al.*, 2014). MoM total hip replacements are performed in younger and more active patients due to the adverse reactions to polyethylene particles generated in metal-on-polyethylene (MoP) bearings (Muller, 1995). However, concerns for the MoM implants become increasingly prominent as adverse reactions to metal debris (ARMD) are widely reported (Matharu *et al.*, 2016; Shulman *et al.*, 2015). Considerable amounts of Co and Cr ions are released into the synovial fluid, with the Co level increasing up to 24,000 ng/μL (approximately 400 μM) in the vicinity of the MoM implants (Davda *et al.*, 2011). Metal ions released into periprosthetic tissues induce cytotoxicity, apoptosis and necrosis, with upregulation of various cytokines and chemokines (Catelas *et al.*, 2001; Fleury *et al.*, 2006; Petit *et al.*, 2004; Queally *et al.*, 2009). The released ions, Co^{2+} and Cr^{3+}, causing issues when using MoM implants, are also frequently reported in patients with MoP bearings with associated adverse effects, including local tissue reactions and pseudotumour formation (Dimitriou *et al.*, 2016; Jennings *et al.*, 2016; Kwon *et al.*, 2016; Pandit *et al.*, 2008; Plummer *et al.*,

2016). Histological evaluation of the synovial tissues from revision hips utilising CoCr alloys frequently reveals an extensive tissue reaction characterised by abundant tissue necrosis and fibrosis with infiltration of immune cells (Campbell *et al.*, 2010). Furthermore, soft tissues – obtained during revision operations – surrounding CoCr components are frequently characterised by massive infiltration of macrophages (Natu *et al.*, 2012). Although total joint replacements are frequently associated with aberrant tissue remodelling (Campbell *et al.*, 2010; Willert *et al.*, 2005), few published studies investigate how the underlying cellular processes are activated by the release of either Co and Cr ions (Madl *et al.*, 2015). Understanding these mechanisms could provide a new means of controlling implant-induced fibrosis and matrix remodelling with the aim of enhancing implant performance.

Investigations of the biological response to implant metal debris and released ions are largely based on cytotoxicity (Behl *et al.*, 2013; Dalal *et al.*, 2012; Papageorgiou *et al.*, 2007), with some studies utilising immune cells to examine the profile of secreted cytokines in response to Co and Cr (Madl *et al.*, 2015). However, few studies examine the sub-toxic effect on fibroblasts, which are responsible for the synthesis and maintenance of the collagenous extracellular matrix (ECM) (Papageorgiou *et al.*, 2007). Accordingly, the current study was designed to examine the effect of Co and Cr ions on the activity of fibroblasts in the form of the mechanical integrity of the ECM. In order to reproduce the synergies between fibroblasts and macrophages in the periprosthetic tissue, the influence of macrophages on the fibrotic response of fibroblasts in the presence of Co and Cr was also examined.

Materials and Methods

Preparation of Co^{2+} and Cr^{3+} solutions

0.1 M stock solutions of Co^{2+} and Cr^{3+} were freshly prepared by dissolving $CoCl_2 \cdot 6H_2O$ (99.5 % purity; Sigma-Aldrich) and $CrCl_3 \cdot 6H_2O$ (98 % purity; Sigma-Aldrich) in sterile H_2O. These solutions were sterilised by filtration through 0.2 μm pore size sterile syringe filter (Merck Millipore). Stock solutions of Co^{2+} and Cr^{3+} were further diluted in cell culture medium to achieve the required experimental concentrations of 100-500 μM for Co^{2+} and 100-800 μM for Cr^{3+}.

Primary culture of human fibroblasts and U937 cells

All cells were maintained at 37 °C in 5 % CO_2 in a humidified atmosphere using the appropriate cell culture medium.

Human dermal fibroblasts (HDFs)

Normal adult HDFs (PromoCell, UK) were grown in Dulbecco's modified Eagle medium (DMEM) (4.5 g/L glucose, Gibco) supplemented with 10 % foetal calf serum (FCS), 0.625 μg/mL amphotericin, 100 IU/mL penicillin and 100 μg/mL streptomycin (all from Sigma-Aldrich). The medium was changed every 3 d until the cells reached 80 % confluency. HDFs between passages 3 and 8 were used for the experiments.

U937 cell line

The U937 cell line (passage 6-25, donation from Dr Akihisa Mitani, Imperial College, London, UK) were cultured in Roswell Park Memorial Institute (RPMI) 1640 medium [1.9 mM L-glutamine, 19 mM 4-(2-hydroxyethyl)-1-piperazineethanesulfonic acid (HEPES); ThermoFisher Scientific] supplemented with 10 % foetal bovine serum (FBS, Sigma-Aldrich), 100 IU/mL penicillin and 100 μg/mL streptomycin. To induce differentiation into adherent macrophage-like cells, U937 cells were treated with 50 ng/mL phorbol 12-myristate 13-acetate (PMA, Sigma-Aldrich) for 48 h. This was followed by a 24 h rest period in complete RPMI 1640 medium prior to further experiments.

Co-culture

Porous plasma-treated polycarbonate inserts (pore size: 3 μm; Transwell, Corning) were used for non-contact co-culture of fibroblasts. HDFs were cultured at 0.4×10^5 cells/well and U937 macrophages at 2×10^5 cells/well in 24-well tissue culture plates. Cells were added to the upper chamber of the Transwell® (Costar) insert, providing a co-culture within each well.

Three-dimensional (3D) culture

Rat tail collagen type I (2 mg/mL, FirstLink, Wolverhampton, UK) was used to fabricate a 3D matrix by collagen fibril self-assembly. The solution containing collagen (1 mg/mL) and 10× minimum essential medium (MEM) (ThermoFisher Scientific) was adjusted to pH 7.4 using 1 M NaOH. A cell suspension was added and the cell-containing collagen mixture was polymerised at 37 °C for 30 min in cell culture plates to create a final cell density of 2×10^5 cells/mL. Serum-free DMEM medium was subsequently added to each well.

Cell viability and proliferation test

A LIVE-DEAD™ Viability/Cytotoxicity Kit (ThermoFisher Scientific) was used to measure cell viability in the presence of Co and Cr ions. HDFs in 96-well tissue culture plates (5×10^3 cells/well for 2D and 2×10^4 cells/well for 3D cultures) were exposed for 6 h to 200, 300 or 500 μM Co^{2+} or 200, 400 or 800 μM Cr^{3+}. Following exposure, supernatants were removed and a 200 μL solution of 1 μM calcein AM and 2 μM ethidium homodimer in phosphate-buffered saline (PBS) was added to each well for 20 min. Then, fluorescence images were captured using a ×10 magnification on a SP2 confocal microscope. Viable cells were stained green with calcein AM (excitation 495 nm, emission 530 ± 12.5 nm), dead cells red with

ethidium homodimer (excitation 528 nm, emission 645 ± 20 nm). Three replicates of each condition were tested, with the assay repeated in three separate experiments.

HDF proliferation was measured using CellTiter 96® AQ_{ueous} One Solution Cell Proliferation Assay (MTS assay, Promega), according to the manufacturer's instructions. HDFs in 96-well tissue culture plates (5×10^3 cells/well for 2D and 2×10^4 cells/well for 3D cultures) were exposed for up to 96 h to 100-500 μM Co^{2+} or 100-800 μM Cr^{3+}. Following exposures, supernatants were aspirated and 100 μL of serum-free DMEM medium containing 10 % CellTiter 96® AQ_{ueous} One Solution Cell Proliferation reagent were added to each well. Plates were incubated for 2 h at 37 °C and the absorbance was measured at 490 nm using an Infinite F50 plate reader (Tecan). Five replicates of each exposure were tested and the assay was repeated in three separate experiments. Cell viability was determined as the percentage of the control cell viability.

3D collagen gel assays

Collagen gel contraction

To measure fibroblast-induced collagen contraction, 0.5 mL of fibroblast-containing collagen solution was added to 24-well cell culture plates and polymerised for 30 min at 37 °C. Then, 0.5 mL of serum-free cell culture medium was added and the gels were incubated for 12 h. Following the incubation, gels containing fibroblasts were gently detached from the wells using fine straight and curved forceps. The medium was aspirated and replaced with culture medium containing Co^{2+} (100, 200 or 300 μM) or Cr^{3+} (100, 200 or 400 μM). The gel contraction was recorded by time-lapse imaging over a 6 h time frame.

Collagen gel stiffness

Gel stiffness was evaluated for untreated samples or samples exposed to 200 μM Co^{2+} as described in the previous section. Shear rheology of fibroblast-containing gels was measured with a strain rotational rheometer (T.A. Instruments, New Caste, UK). Storage modulus was measured over a strain range of 0.2-2 % at a fixed angular frequency of 0.5 rad/s and a temperature of 21 °C.

Immunofluorescence

Co/Cr-treated fibroblasts were fixed with 4 % paraformaldehyde (Sigma-Aldrich), washed and permeabilised with 0.5 % Triton X-100 (Sigma-Aldrich) and rinsed 3 times with PBS. Non-specific binding sites were blocked with 1 % bovine serum albumin (BSA) in PBS. Cells were labelled for α-smooth muscle actin (α-SMA) by incubation overnight at 4 °C with a mouse monoclonal anti-α-SMA primary antibody (1 : 400, Abcam). Then, cells were washed and incubated for 1 h at room temperature in Alexa 488 conjugated anti-mouse IgG as a secondary antibody (1 : 1000, ThermoFisher Scientific). To label the cellular F-actin, fixed fibroblasts in collagen gel were incubated for 30 min with 200 μL of rhodamine-conjugated phalloidin (Molecular Probes) in a humidified chamber at room temperature in the dark. Before imaging, cell nuclei were stained by incubation with 5 μg/mL 4',6-diamidino-2-phenylindole (DAPI; Dojindo, Rockville, MD, USA) followed by three PBS rinses. Slides were visualised with a fluorescence microscope (Leica SP2) utilising a ×10 and ×63 objective.

Transwell® cell migration assay

Cell migration was investigated using 6.5 mm Transwell® chambers with 8 μm pores (Costar). Briefly, 5×10^4 HDFs in serum-free DMEM were added to the upper chamber of the insert. The lower chamber was filled with 600 μL of DMEM supplemented with 10 % FBS to encourage cell migration towards the FBS chemotactic gradient. Cell migration was analysed over a 6 h period in the presence of 200 μM Co^{2+} in the medium. After 6 h, the migrated cells attached to the bottom surface of the insert were fixed, stained with crystal violet and counted with an inverted microscope utilising a ×10 objective.

Atomic force microscopy (AFM)

The stiffness of HDFs was measured by AFM (Kreplak, 2006) using the Advanced Quantitative Imaging mode on a JPK NanoWizard 4 system (Bruker Nano GmbH, Berlin, Germany) in combination with an inverted microscope (Axio Observer Z1, Zeiss). Cantilevers (HYDRA6R, AppNano, Mountain View, CA, USA) were calibrated by measuring the sensitivity against a stiff polystyrene substrate and fitting the resonance peak in the thermal noise spectrum to determine the spring constant (approximately 0.08 N/m). A region of interest of 100 × 100 μm was selected to cover an entire cell. Indentations were performed in a format of 32 × 32 μm at a loading/unloading speed of 50 μm/s, which minimised cell movement during scanning without compromising the resolution. All the AFM experiments were carried out at 37 °C in FBS-free medium. Force-indentation curves were further processed in JPK data processing software, which involved background subtraction, height correction and fitting with a modified Hertzian model. A Poisson's ratio of 0.5 was assumed. Young's modulus ranging from 1 kPa to 100 kPa were extracted and a mean value determined to estimate the overall stiffness of a cell.

Traction force measurement

22 mm coverslips (Corning) were treated with hexamethyldisilazane (HMDS, VWR) overnight, rinsed in distilled water and air-dried. A gel solution of 5 % containing acrylamide (Biorad), 0.25 % bis-acrylamide (Biorad), 0.05 % ammonium persulphate (10 % APS stock, Sigma-Aldrich), 0.1 % 1, 2-Bis (dimethylamino) ethane (TEMED, Sigma-Aldrich) and carboxylate-modified beads (fluorescent red, diameter 0.2 μm, 1 % volume

concentration, ThermoFisher Scientific) was applied to the hydrophobic coverslips. After 15 min polymerisation at room temperature, the gel was activated under UV light for 30 min with 1 mg/mL of the heterobifunctional cross-linker Sulfo-SANPAH (Sigma-Aldrich) and rinsed 5 times with distilled water. Then, the gels were coated with 0.2 mg/mL type I rat tail collagen. Fibroblasts at a density of 3×10^4 cells/well were plated on the coverslips in a serum-free DMEM and subjected to Co treatment (200 μM) for 6 h prior to imaging (LS720 Microscope, Lumascope) in a humid incubator. Bright-field and 525 nm image stacks were acquired at each position. After imaging, fibroblasts were lysed with 1 % sodium dodecyl sulphate (SDS) with positions re-imaged. A custom-built analysis pipeline implemented in LabVIEW (National Instruments, Austin, TX, USA) was used to measure the traction forces as previously described (Gavara *et al.*, 2006).

ROS measurement

ROS formation was measured using 5-(and 6-)-chloromethyl-2′7′-dichlorodihydrofluorescein diacetate (CM-H_2DCFDA, ThermoFisher Scientific). HDFs in collagen gels (2×10^4 cells/gel) were cultured in black 96-well cell culture plates with a clear bottom. After 6 h exposure to 100-300 μM Co^{2+}, the supernatant was aspirated and the cells were washed with warm PBS. 1 μM (100 μL) CM-H_2DCFDA in Hanks' balanced salt solution (HBBS) was added to the gels that were subsequently incubated for 30 min at 37 °C in the dark. Fluorescence was measured at an excitation of 485 ± 20 nm and an emission of 528 ± 20 nm using a microplate reader (BMG Nova Star, BMG LABTECH, Aylesbury, UK).

Hydroxyproline collagen assay

To measure the amount of hydroxyproline released in the cell culture medium, HDFs were exposed for 24 h to 200 μM Co^{2+} or 400 μM Cr^{3+} with or without the presence of U937 macrophages. The culture medium was collected and hydrolysed in 6 N HCl for 24 h at 105 °C. The amount of 4-hydroxyproline in the hydrolysate was determined at a wavelength of 570 nm with a microplate reader (BMG Nova Star, BMG LABTECH) using the conventional colorimetric method (Reddy and Enwemeka, 1996).

Protein extraction and immunoblotting

All lysis buffers were supplemented with 1 % protease inhibitor (Sigma-Aldrich). Protein extracts were resolved using gradient precast SDS-polyacrylamide gel electrophoresis (Biorad) and electro-transferred onto a nitrocellulose membrane by using Trans-Blot® Turbo™ Transfer System (Biorad) for immunoblot analysis. Antibody probing was performed as per manufacturers' instructions. Anti-myosin light chain (MLC) (phospho S20) antibody (1 : 1,000, Abcam) and anti-GAPDH antibody (1 : 2,000, Abcam) were used. Secondary antibodies, either IRDye® 800CW goat anti-mouse IgG (LI-COR) or IRDye® 800CW goat anti-rabbit IgG (LI-COR), were used with dilution of 1 : 10,000. Specific protein bands were detected using Odyssey® CLx Imaging System (LI-COR).

Data analysis and statistics

All data were expressed as the mean ± standard error of the mean (SEM) of at least three independent experiments. Statistical differences between control and experimental groups were analysed with Mann-Whitney U test (SPSS Inc). A value of $p < 0.05$ was considered to be statistically significant.

Results

Effect of Co^{2+} and Cr^{3+} on human dermal fibroblasts viability and proliferation

The viability and proliferation of HDFs in the presence of either Co^{2+} and Cr^{3+} was assessed in both 2D and 3D gel cultures. Following 6 h of exposure, both Co^{2+} (200-500 μM) and Cr^{3+} (200-800 μM) yielded minimal effects on the cell viability in either 2D or 3D (Fig. 1**a**, quantification of cell viability following treatment are not shown). The effect of Co^{2+} and Cr^{3+} on the proliferative capacity of fibroblasts in 2D, investigated by using a CellTiter MTS cell proliferation assay, showed that Co^{2+} had no obvious effects on fibroblast proliferation over the first 24 h of treatment (Fig. 1**b**). After 48 h of exposure, 100, 200 and 300 μM Co^{2+} transiently increased (although the increase was not statistically significant) the number of fibroblasts by around 5, 5 and 8 %, respectively, before returning to control levels. However, this effect was not seen when fibroblasts were subjected to Co^{2+} in 3D collagen matrices (Fig. 1**c**). In addition, 500 μM Co^{2+} significantly decreased the fibroblast proliferation by around 20 % when compared with untreated cells at 48 and 72 h. 300 and 500 μM Co^{2+} also supressed cell proliferation in 3D collagen matrices after 72 h (Fig. 1**c**). By contrast, Cr^{3+} at concentrations ranging from 200 to 800 μM had no statistically significant effect on fibroblast proliferation over 72 h of treatment (Fig. 1**d**,**e**). Based on these results, the effects of Co^{2+} and Cr^{3+} on fibroblast behaviour were investigated by using 200 μM Co^{2+} and 400 μM Cr^{3+}, which had no significant effect on either fibroblast viability or proliferation.

Remodelling of HDF-seeded collagen gels following exposure to Co^{2+}

To investigate the direct impact of Co^{2+} on fibroblast functionality, fibroblasts were cultured in type I collagen gels and their morphology was evaluated following 6 h exposure to either 200 μM Co^{2+} or 400 μM Cr^{3+}. Treatment with Cr^{3+} had no detectable effect on fibroblast morphology, with cells retaining an elongated spindle-like appearance within the collagen matrices, similar to that of untreated cells. By contrast, Co^{2+} treatment caused a contracted

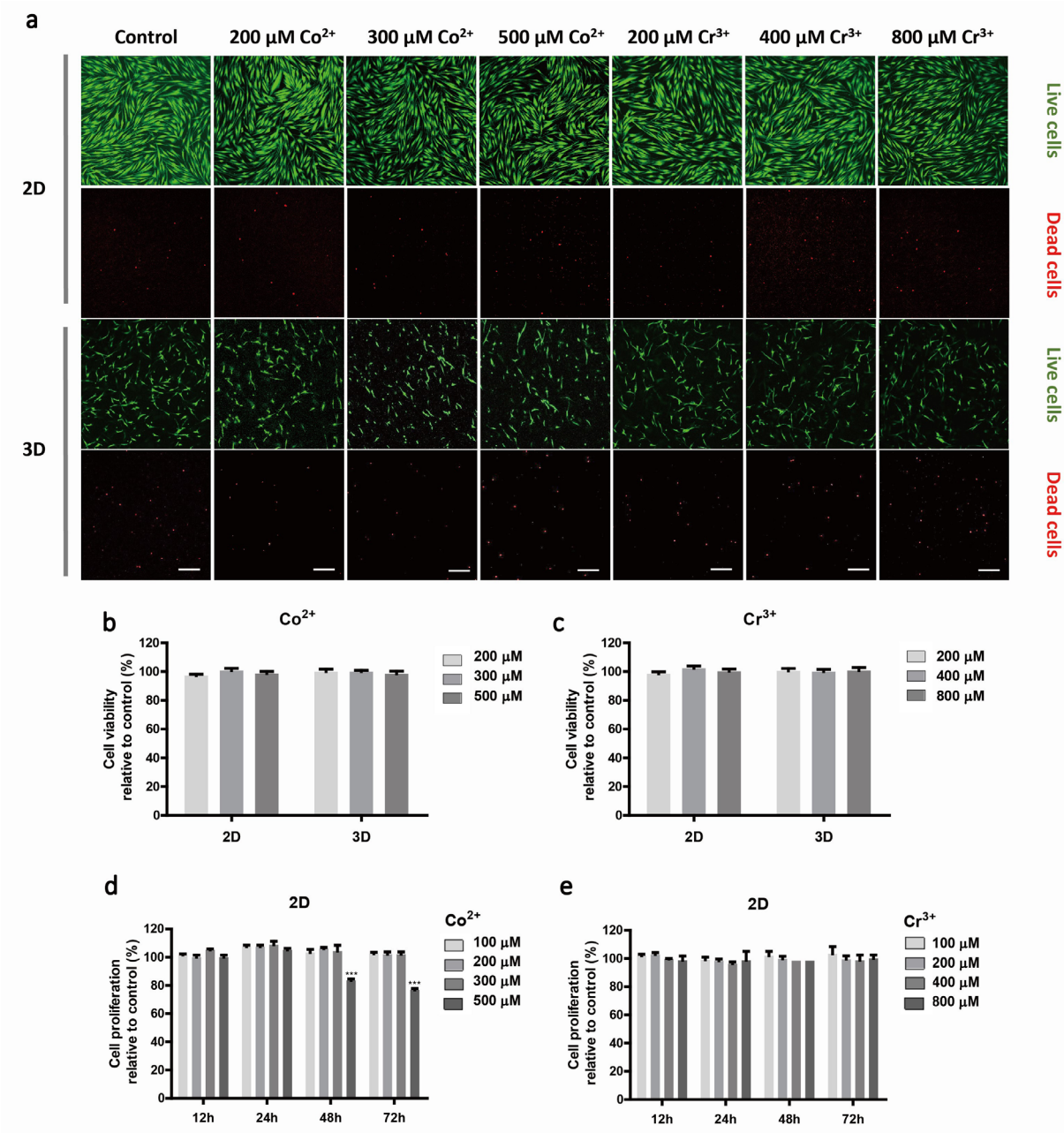

Fig. 1. HDFs viability and proliferation assessed by live/dead assay and MTS assay. (**a**) Representative fluorescence images showing staining of live (green) and dead (red) cells in 2D and 3D culture following exposure to Co^{2+} and Cr^{3+} (20× magnification; scale bar: 100 µm). The effect of (**b**,**c**) Co^{2+} and (**d**,**e**) Cr^{3+} on HDFs proliferation capacity when grown in 2D tissue culture plates or 3D collagen matrices. Data represent mean + SEM, $n = 9$ from 3 independent experiments, with 5 replicates for each condition. Mann-Whitney U test was used to compare differences between control and treated group; * $p < 0.05$; *** $p < 0.001$.

morphology, with an increased formation of actin stress fibres (Fig. 2**a**) and a reduced fibroblast length (Fig. 2**b**).

Next, the effect of Co on the fibroblasts' ability to contract and remodel their surrounding matrix was investigated. Over 6 h of exposure, Co^{2+} enhanced collagen gel contraction in a time-dependent manner whilst untreated cells showed a negligible contraction (Fig. 2**c**,**d**): the collagen gels were contracted by nearly 50 % within the first hour following exposure to Co^{2+} (100-300 µM). The higher dose of Cr^{3+} (300 µM) triggered a more rapid contraction of the collagen matrices with significant differences at 30 min as compared to 100 µM Co^{2+}. By contrast, 100-400 µM Cr^{3+} treatment showed no statistically significant effect on collagen gel contraction (Fig. 2**c**,**d**, data only shown for 400 µM Cr^{3+}). The storage modulus of the cell-seeded collagen gels was independent of the strain magnitude (Fig. 2**e**). Cells treated for 6 h with 200 µM Co^{2+} remodelled their collagen matrix resulting in a statistically significant increase in storage modulus from a mean value of 6.9 ± 0.74 Pa in untreated constructs to 12.5 ± 1.3 Pa in treated constructs (Fig. 2**f**). Cr^{3+} had no significant effect on

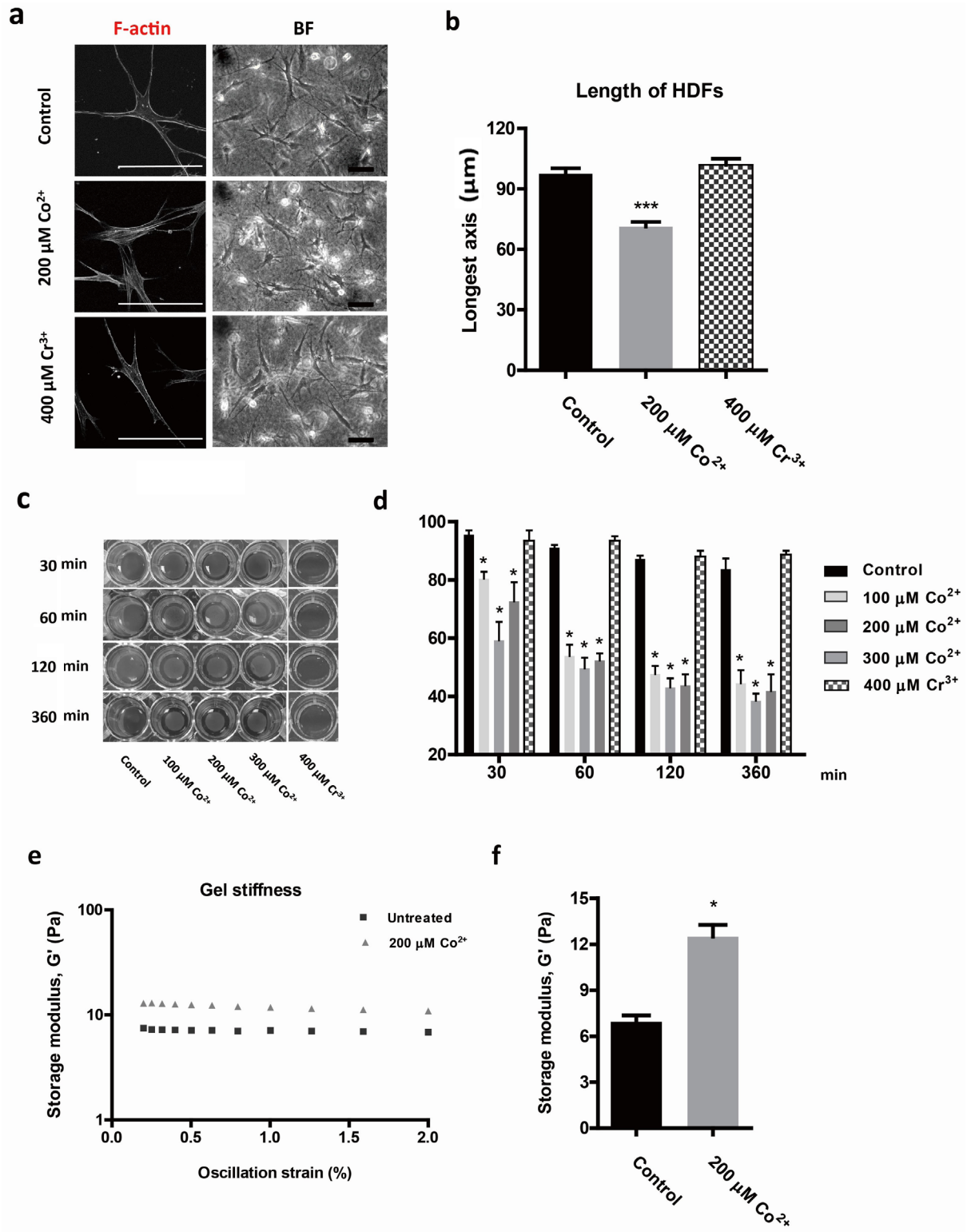

Fig. 2. Co^{2+} triggered fibroblasts-populated collagen gel remodelling. (**a**) F-actin staining of human fibroblasts grown in 3D collagen gels; scale bar: 100 μm. (**b**) Bars show quantification of the longest distance of fibroblast grown in 3D collagen gels. Bars represent mean + SEM; $n = 50$ individual cells from three experimental repeats. Mann-Whitney U test was used to compare differences between control and treated group; *** $p < 0.001$. (**c**) HDFs-induced gel contraction assay. Images show HDFs-induced contraction of collagen I matrices remodelling over 6 h of treatment; (**d**) quantification of Co/Cr-induced collagen gel contraction relative to control; bars indicate mean + SEM; Mann-Whitney U test was used to compare differences between control and treated group; $n = 6$ from three experimental repeats; * $p < 0.01$. (**e**) Matrix stiffness of collagen gel with or without 200 μM Co^{2+} treatment. (**f**) Storage modulus (G′) of collagen I measured by shear rheology after 6 h of fibroblasts remodelling; bars represent mean + SEM; Mann-Whitney U test was used to compare differences between control and treated group; $n = 6$ from three experimental repeats; * $p < 0.01$.

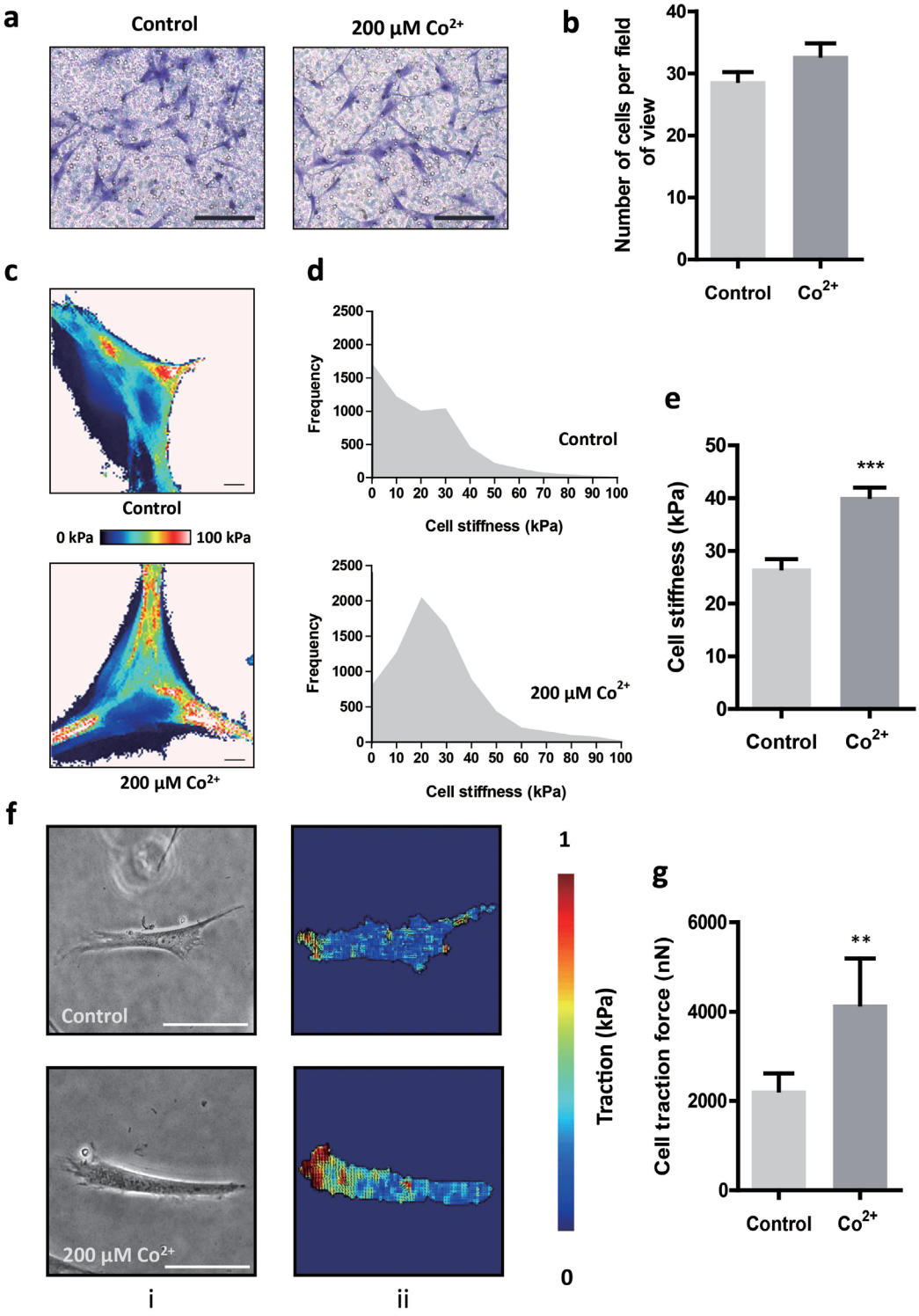

Fig. 3. Altered cellular contractile forces and cell stiffness of Co-treated fibroblasts. (**a**) Trans-well migration assay showing the effect of Co^{2+} on fibroblast migration. Scale bar: 200 µm. (**b**) Quantifications of the migration assay is based on three independent experiments. Values represent mean + SEM; $n = 30$ from three independent experiments; for each experiment, 10 random fields were imaged for each treatment. (**c**) Representative images showing the Young's modulus of a control and of a Co^{2+}-treated fibroblast (scale bar: 10 µm); (**d**) associated density plot showing distribution of the measured stiffness for values of individual locations of measurement within the physiological range of 0 kPa to 100 kPa. (**e**) Quantification of the mean cell stiffness of control and of Co^{2+}-treated fibroblasts, $n = 30$, Mann-Whitney U test; *** $p < 0.001$. (**f**) Contractile forces of a representative control and Co^{2+}-treated fibroblast. Bright field images of individual cell (i) and corresponding stress magnitude maps (ii). Scale bar: 50 µm. (**g**) Quantification of cellular contractile force of fibroblasts from control and untreated cells; $n = 30$; Mann-Whitney U test; ** $p < 0.01$.

the stiffness of fibroblast-populated collagen gels (data not shown).

Co^{2+}-induced fibroblast contractility was associated with altered biomechanical properties dependent on ROS production

Effects of Co on fibroblast migration and biomechanical properties

The effect of Co on cell migration was examined, based on previous studies suggesting that collagen gel contraction may be due to an enhanced cell motility (Andujar *et al.*, 1992). However, the current study revealed no significant effect of 200 μM Co^{2+} on fibroblast 3D migration, when using a trans-well migration assay (Fig. 3**a**,**b**).

The results obtained motivated a further investigation as to whether the altered cellular contractility and cytoskeleton organisation of Co^{2+}-treated fibroblasts were associated with changes in the biomechanical properties of fibroblasts. Using

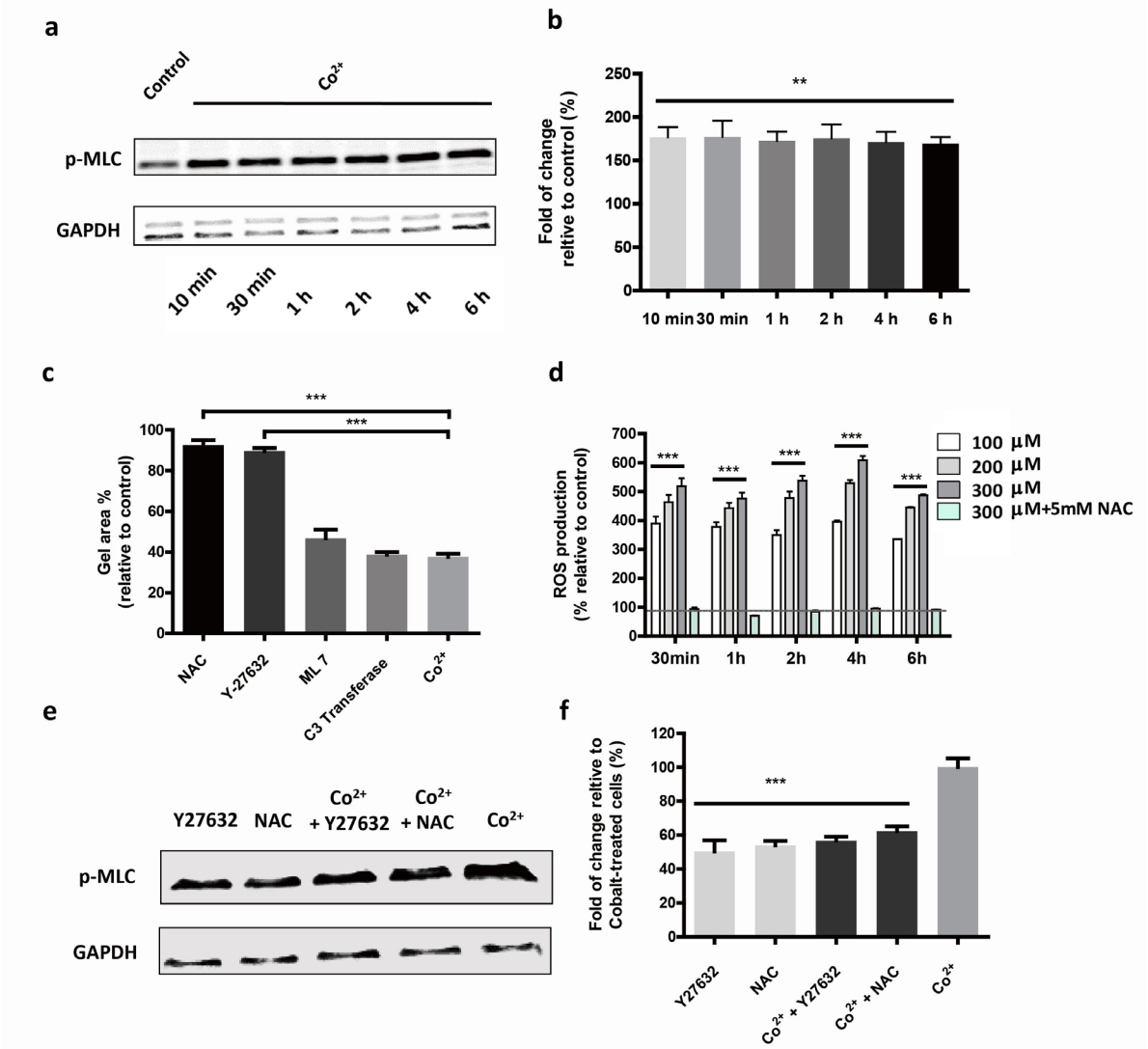

Fig. 4. Co^{2+}-induced fibroblast activation was dependent on ROS production. (**a**) Phosphorylation of MLCs stimulated by 200 μM Co^{2+} over 6 h of treatment. (**b**) Quantification of the phosphorylation of MLCs stimulated by 200 μM Co^{2+} over time. Statistically significant differences are indicated relative to untreated control based on Mann-Whitney U test. Values represent mean + SEM; $n = 6$ from three independent experiments; *** $p < 0.001$. (**c**) The effects of the antioxidant NAC, ROCK1 inhibitor Y-27632, MLCK inhibitor ML-7 and RhoA inhibitor C3 transferase on 200 μM Co^{2+}-mediated fibroblast-induced collagen gel contraction. Mann-Whitney U test. Values represent mean + SEM; *** indicates difference from cell only treated by Co^{2+}, $n = 6$ from 3 independent experiments (2 replicates/experiment); *** $p < 0.01$. (**d**) ROS formation stimulated by 100-300 μM Co^{2+} over 6 h of treatment and inhibition of ROS formation by NAC. Mann-Whitney U test. Values represent mean + SEM; $n = 9$ from 3 independent experiments (3 replicates/experiment); *** indicates difference from untreated cells, *** $p < 0.001$. (**e**) The effects of the antioxidant NAC and ROCK1 inhibitor Y-27632 on the phosphorylation of MLCs of fibroblast treated with 200 μM Co^{2+}. (**f**) Quantification of the phosphorylation of MLCs when Y-27632 and NAC were added to the fibroblasts treated with 200 μM Co^{2+}. Mann-Whitney U test. Values represent mean + SEM; $n = 6$ from 3 independent experiments (2 replicates/experiment); *** indicates difference from Co^{2+}-treated cells, *** $p < 0.001$.

AFM and traction force microscopy, cell stiffness and contractile forces were assessed, respectively. When compared with untreated cells, Co^{2+}-treated fibroblasts showed increased median stiffness, which was characterised by statistically significant differences in elastic moduli ($p < 0.001$, Fig. 3**c**-**e**). Representative AFM images of the cell stiffness measured from a control and a Co^{2+}-treated fibroblast are provided in Fig. 3**c**, with the frequency distribution of the stiffness illustrated in Fig. 3**d**. According to the AFM images (Fig. 3**c**), the stiffest region of the Co^{2+}-treated fibroblast mainly corresponded to the periphery of the cell, which indicated the higher density, cross-link content and better alignment of the actin at the edge of the cell as compared with untreated cells. Additionally, fibroblasts exposed to Co^{2+} exhibited a near 2-fold increase in cellular contractile force ($p < 0.01$, Fig 3**f**,**g**).

Co^{2+} promoted phosphorylation of MLC and ROS production

The cellular contractile state is governed by the actin-myosin-mediated motor activity (Ennomani *et al.*, 2016). Non-muscle myosins are regulated by the cyclic phosphorylation and activation of the MLCs (Moussavi *et al.*, 1993; Vicente-Manzanares *et al.*, 2009). In the present study, 200 μM Co^{2+} induced a sustained enhancement in phosphorylation of MLCs over 6 h of treatment. This increase was approximately 80 % 10 min after the initiation of the Co^{2+} treatment (Fig. 4**a**,**b**). Phosphorylation of myosin is catalysed either by the MLC kinase (MLCK) or by the Rho-associated coiled-coil-forming kinase (ROCK) (Fukata *et al.*, 2001). The MLCK inhibitor ML-7 (10 μM, Sigma-Aldrich) did not have any inhibitory effect, while pre-treatment with the ROCK1 inhibitor Y-27632 (10 μM, Sigma-Aldrich) completely prevented the

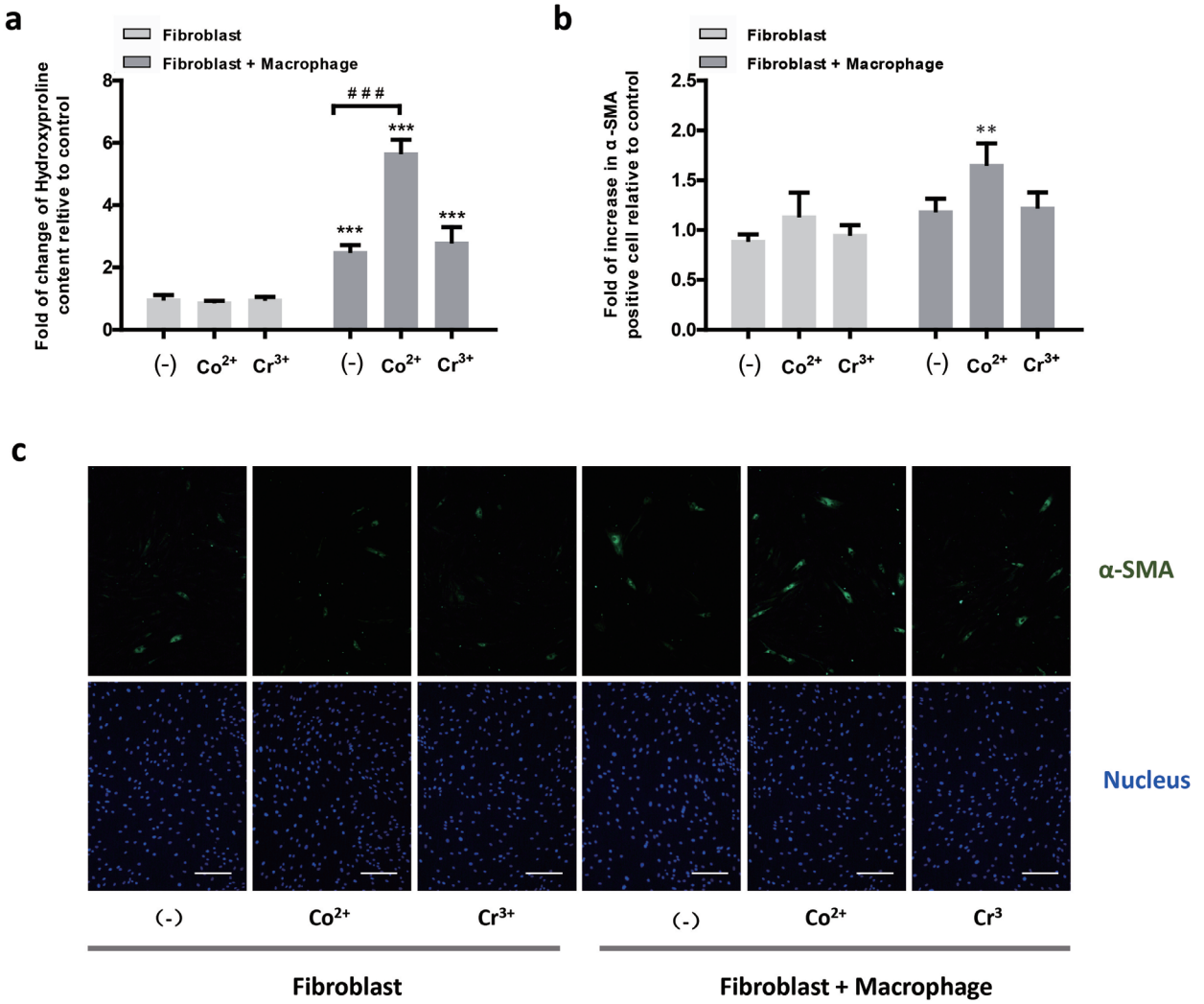

Fig. 5. Co^{2+} stimulated the release of pro-fibrotic signals from macrophages. (**a**) Fold of change in the amount of hydroxyproline content measured in the culture medium from fibroblast when treated with 200 μM Co^{2+}, 400 μM Cr^{3+} with or without U937 macrophages or co-culture without treatments. Values represent mean + SEM; $n = 9$ from 3 independent experiments (3 replicates/experiment). (**b**) Fold of change in the percentages of α-SMA-positive fibroblasts with different treatments as described in (**a**); $n = 30$ from 3 independent experiments; 10 random fields were imaged for each treatment in each experiment. * indicates significant difference from untreated fibroblasts and # indicates difference between untreated co-culture cells and Co^{2+}-treated co-culture cells; ** $p < 0.01$, ###/*** $p < 0.001$; Mann-Whitney U test. (**c**) Representative images of fibroblasts with α-SMA marker stained in each group; green: α-SMA; blue: nucleus; scale bar: 200 μm.

fibroblast-induced collagen gel contraction. ROCK1 is activated by the small GTPase Rho*A (*Tang *et al.*, 2012); therefore, the activity of RhoA was inhibited by treating fibroblasts during Co^{2+} exposure with the cell permeable RhoA inhibitor C3 transferase (2 μg/mL, Cytoskeleton, Colorado, CO, USA). However, supressing RhoA activity did not prevent collagen gel contraction (Fig. 4**c**). Hence, Co^{2+} did not induce fibroblast contraction *via* RhoA/ROCK1 signalling pathway, although ROCK activity was still required during this process.

Exposure to Co^{2+} induces ROS formation (Chandel *et al.*, 1998; Harris and Shi, 2003; Zou *et al.*, 2001). When cells were pre-treated for 30 min with a ROS inhibitor in the form of the antioxidant N-acetyl-cysteine (NAC, 5 mM, Sigma-Aldrich), Co^{2+}-induced fibroblast contractility was completely prevented (Fig. 4**d**). Further, treatment with NAC reduced the phosphorylation of MLCs to base levels similar to that in untreated cells (Fig. 4**e**,**f**). In summary, these results suggested that Co^{2+} induced the activation of the fibroblast contractile phenotype by promoting MLC phosphorylation mediated through the generation of ROS.

Co^{2+} stimulated the release of pro-fibrotic signals from macrophages

To investigate whether Co^{2+}-induced fibroblast contraction was accompanied by an enhanced collagen production, the amount of hydroxyproline secreted by the fibroblasts was measured following different treatments (Myllyharju and Kivirikko, 2004). Co^{2+} or Cr^{3+} alone did not have any obvious effect on pro-collagen production (Fig. 5**a**). However, when U937 macrophages were included in the culture and exposed to Co^{2+} or Cr^{3+}, the amount of hydroxyproline content in the culture medium was significantly increased. Interestingly, co-cultures of fibroblasts and macrophages treatment with Co^{2+} induced a synergistic response with an increase in hydroxyproline release nearly 5 times more than in fibroblasts alone (Fig. 5**a**). Co-cultures treated with Cr^{3+} did not exhibit this synergistic effect.

α-SMA expression, a marker of contractile and collagen-producing fibroblasts (Hinz, 2010), was also determined to assess the activation of cells exposed to Co^{2+} or Cr^{3+}. The number of α-SMA-positive fibroblasts was significantly upregulated when macrophages and fibroblasts were co-cultured in the presence of Co^{2+} (Fig. 5**b**,**c**). These results indicated that Co^{2+} stimulated the release of pro-fibrotic signals from macrophages, which enhanced the fibrotic response of fibroblasts. In contrast, Cr^{3+} induced no significant effects.

Discussion

Clinical reports highlight the presence of soft tissue responses, including abundant tissue necrosis and inflammatory fibrosis, in some patients with MoM implants (Bosker *et al.*, 2015). This adverse tissue response to metals can also occur in non-MoM hip prostheses, when abnormal metal-metal contact occurs, for example when there is impingement of the acetabula cup on the trunnion (Jennings *et al.*, 2016; Kwon *et al.*, 2016). However, how the metal debris, whether in particulate or ionic form, causes the destruction of soft tissue remains unclear. To elucidate this mechanism, the effect of Co and Cr on human fibroblasts, the key cells involved in the fibrotic response, was investigated. No synergistic effect of Co and Cr ions on cell viability is shown in previous studies (Shah *et al.*, 2015), therefore, this matter was not explored.

The results of the present study revealed that Co^{2+}, but not Cr^{3+}, significantly enhanced the fibroblast capability of contracting the ECM (tested by using type I collagen gels). The enhanced contractility was associated with an alteration in both cytoskeletal and biomechanical properties. Furthermore, Co^{2+} stimulated the release of pro-fibrotic signals from the macrophages, which subsequently promoted the collagen synthesis and increased the number of α-SMA-positive fibroblasts.

Both 2D and 3D models were used to study the effects of Co^{2+} and Cr^{3+} at non-cytotoxic concentrations on human fibroblasts. An increased contraction of fibroblast-populated collagen gels was observed after treatment with Co^{2+}. This response associated with changes in fibroblast cytoskeleton and gradually resulted in stiffer collagen matrices. Using AFM and traction force microscopy, it was shown that the altered fibroblast contractility was associated with changes in mechanical properties. Co^{2+} exposure produced a significant increase in cell stiffness and enhanced contractile forces. This confirmed previous observations according to which the biomechanical properties of fibroblasts serve as a key regulator of the cell's ability to organise the ECM (Humphrey *et al.*, 2014; Rhee, 2009; Rhee and Grinnell, 2007). As an example, fibroblasts are capable of dynamically shaping the ECM due to alteration in their cytoskeleton, consequently mediating the onset and progression of cancer (Alkasalias *et al.*, 2017).

Co^{2+} drove the contraction of fibroblasts by regulating MLC phosphorylation, which could be abrogated by a ROS scavenger. Co^{2+} leads to the generation of ROS in a range of cell types (Leonard *et al.*, 1998). The present results indicated, for the first time, that this Co^{2+}-induced ROS formation also played a critical role in ECM modulation by fibroblasts.

Fibroblast activation is followed by differentiation into myofibroblasts (MFs), particularly observed in conditions requiring tissue remodelling, such as wound healing and fibrosis (Eckes *et al.*, 2000). MFs form contractile stress fibres and express *de novo* α-SMA (Tomasek *et al.*, 2002). The present study indicated that Co^{2+} exposure led to differentiation of HDFs by enhancing α-SMA expression, an observation only evident during co-culture with

macrophages. The co-culture also produced a Co^{2+}-induced collagen (in form of hydroxyproline) release from fibroblasts. Macrophages play a critical role in disease progression and in mediating the interplay between tissue and biomaterials. Immune cells are affected by matrix stiffness, *e.g.* stiffer substrates enhance both neutrophil transmigration (Stroka and Aranda-Espinoza, 2011) and release of pro-inflammatory cytokines by macrophages stimulated with lipopolysaccharide (Blakney *et al.*, 2012). These observations suggest that immune cells probe and sense an alteration in the mechanical properties of the extracellular environment, hence could interact with the altered matrices through fibroblasts inducing contraction. This could explain the enhanced pro-fibrotic response of Co^{2+}-treated fibroblasts during macrophage co-culture.

Macrophages are capable of not only directly activating fibroblasts by releasing transforming growth factor-β1 (TGF-β1) and platelet-derived growth factor (PDGF) (Bonner *et al.*, 1991; Wahl *et al.*, 1990), but also controlling ECM turnover by regulating the balance of matrix metalloproteinases and their inhibitors (Fallowfield *et al.*, 2007; Hironaka *et al.*, 2000; Madala *et al.*, 2010). Moreover, macrophages exacerbate fibrogenesis by producing chemokines that recruit fibroblasts and other inflammatory cells (Wynn, 2007). Furthermore, Co-treated macrophages also promote cellular α-SMA expression, which is associated with upregulated collagen synthesis by fibroblasts as compared with α-SMA-negative fibroblasts. Co stimulates macrophages to release a range of inflammatory mediators, such as interleukin 1β (IL-1β) and tumour necrosis factor-α (TNF-α) (Goodman, 2007), which can affect ECM turnover and tissue homeostasis.

Total joint replacements may trigger unusual tissue remodelling (Campbell *et al.*, 2010; Willert *et al.*, 2005) activated by the release of metal, in particular Co ions (Savarino *et al.*, 2002). The control of ROS can influence implant-induced fibrosis and matrix remodelling and, thereby, enhance implant performance, as evidenced by the co-culture of fibroblasts with macrophages (Fig. 5). In the present study, the effects of Co on fibroblast and macrophage-mediated ECM remodelling was explored. Activation of fibroblasts by Co, which was exacerbated in the presence of macrophage, provided a mechanistic explanation for the excessive ECM protein deposition and aberrant matrix remodelling, with intensive infiltration of immune cells, observed in the patients with MoM hip replacement implants. In addition, ECM remodelling could also impact immune cells' behaviour and give rise to an enhanced inflammatory response, *e.g.* adverse tissue reaction in hip replacement. Patients with upregulated Co ions level need to be aware of a potential fibrosis response.

The limitation of this study was the use of an established fibroblast cell line rather than primary human synovial fibroblasts, which might affect the direct translation of *in vitro* findings to the clinical setting. The effects induced by Co would need to be further investigated in fibroblasts from patients following the implantation of MoM devices.

Conclusions

Co^{2+} altered cytoskeleton, contractile forces and cell stiffness of the fibroblast, inducing a profibrotic state, which was mediated by the production of ROS. Moreover, the profibrotic effect could be further enhanced by the presence of macrophages. In the light of these results, Co and macrophage acted synergistically to affect the functional properties of fibroblasts and ECM homeostasis. However, further studies are needed to determine the key mediators that govern these fibrotic reactions.

Acknowledgement

The authors are grateful to the China Scholarship Council (CSC) for their support to Jing Xu, Xiaoli Zhang and the grant from BBSRC (BB/N018532/1) for the support to Núria Gavara. We are grateful to Capital investment fund from the Institute of Bioengineering at Queen Mary University of London that was used to purchase the BioAFM used in this study.

References

Alkasalias T, Alexeyenko A, Hennig K, Danielsson F, Lebbink RJ, Fielden M, Turunen SP, Lehti K, Kashuba V, Madapura HS, Bozoky B, Lundberg E, Balland M, Guven H, Klein G, Gad AK, Pavlova T (2017) RhoA knockout fibroblasts lose tumor-inhibitory capacity *in vitro* and promote tumor growth *in vivo*. Proc Natl Acad Sci U S A **114**: E1413-E1421.

Andujar MB, Melin M, Guerret S, Grimaud JA (1992) Cell-migration influences collagen gel contraction. J Submicrosc Cytol Pathol **24**: 145-154.

Behl B, Papageorgiou I, Brown C, Hall R, Tipper JL, Fisher J, Ingham E (2013) Biological effects of cobalt-chromium nanoparticles and ions on dural fibroblasts and dural epithelial cells. Biomaterials **34**: 3547-3558.

Blakney AK, Swartzlander MD, Bryant SJ (2012) The effects of substrate stiffness on the *in vitro* activation of macrophages and *in vivo* host response to poly(ethylene glycol)-based hydrogels. J Biomed Mater Res A **100**: 1375-1386.

Bonner JC, Osorniovargas AR, Badgett A, Brody AR (1991) Differential proliferation of rat lung fibroblasts induced by the platelet-derived growth factor-AA, factor-AB, and factor-BB isoforms secreted

by rat alveolar macrophages. Am J Respir Cell Mol Biol **5**: 539-547.

Bosker BH, Ettema HB, Van Rossum M, Boomsma MF, Kollen BJ, Maas M, Verheyen CC (2015) Pseudotumor formation and serum ions after large head metal-on-metal stemmed total hip replacement. Risk factors, time course and revisions in 706 hips. Arch Orthop Trauma Surg **135**: 417-425.

Campbell P, Ebramzadeh E, Nelson S, Takamura K, De Smet K, Amstutz HC (2010) Histological features of pseudotumor-like tissues from metal-on-metal hips. Clin Orthop Relat Res **468**: 2321-2327.

Catelas I, Petit A, Zukor DJ, Huk OL (2001) Cytotoxic and apoptotic effects of cobalt and chromium ions on J774 macrophages – implication of caspase-3 in the apoptotic pathway. J Mater Sci Mater Med **12**: 949-953.

Chandel NS, Maltepe E, Goldwasser E, Mathieu CE, Simon MC, Schumacker PT (1998) Mitochondrial reactive oxygen species trigger hypoxia-induced transcription. Proc Natl Acad Sci U S A **95**: 11715-11720.

Dalal A, Pawar V, McAllister K, Weaver C, Hallab NJ (2012) Orthopedic implant cobalt-alloy particles produce greater toxicity and inflammatory cytokines than titanium alloy and zirconium alloy-based particles *in vitro*, in human osteoblasts, fibroblasts, and macrophages. J Biomed Mater Res A **100**: 2147-2158.

Davda K, Lali FV, Sampson B, Skinner JA, Hart AJ (2011) An analysis of metal ion levels in the joint fluid of symptomatic patients with metal-on-metal hip replacements. J Bone Joint Surg Br **93**: 738-745.

Dimitriou D, Liow MHL, Tsai TY, Leone WA, Li GA, Kwon YM (2016) Early outcomes of revision surgery for taper corrosion of dual taper total hip arthroplasty in 187 patients. J Arthroplasty **31**: 1549-1554.

Eckes B, Zigrino P, Kessler D, Holtkötter O, Shephard P, Mauch C, Krieg T (2000) Fibroblast-matrix interactions in wound healing and fibrosis. Matrix Biol **19**: 325-332.

Ennomani H, Letort G, Guerin C, Martiel JL, Cao WX, Nedelec F, De la Cruz EM, Thery M, Blanchoin L (2016) Architecture and connectivity govern actin network contractility. Curr Biol **26**: 616-626.

Fallowfield JA, Mizuno M, Kendall TJ, Constandinou CM, Benyon RC, Duffield JS, Iredale JP (2007) Scar-associated macrophages are a major source of hepatic matrix metalloproteinase-13 and facilitate the resolution of murine hepatic fibrosis. J Immunol **178**: 5288-5295.

Fleury C, Petit A, Mwale F, Antoniou J, Zukor DJ, Tabrizian M, Huk OL (2006) Effect of cobalt and chromium ions on human MG-63 osteoblasts *in vitro*: morphology, cytotoxicity, and oxidative stress. Biomaterials **27**: 3351-3360.

Fukata Y, Amano M, Kaibuchi K (2001) Rho-Rho-kinase pathway in smooth muscle contraction and cytoskeletal reorganization of non-muscle cells. Trends Pharmacol Sci **22**: 32-39.

Gavara N, Sunyer R, Roca-Cusachs P, Farre R, Rotger M, Navajas D (2006) Thrombin-induced contraction in alveolar epithelial cells probed by traction microscopy. J Appl Physiol **101**: 512-520.

Goodman SB (2007) Wear particles, periprosthetic osteolysis and the immune system. Biomaterials **28**: 5044-5048.

Harris GK, Shi XL (2003) Signaling by carcinogenic metals and metal-induced reactive oxygen species. Mutat Res **533**: 183-200.

Hinz B (2010) The myofibroblast: paradigm for a mechanically active cell. J Biomech **43**: 146-155.

Hironaka K, Sakaida I, Matsumura Y, Kaino S, Miyamoto K, Okita K (2000) Enhanced interstitial collagenase (matrix metalloproteinase-13) production of Kupffer cell by gadolinium chloride prevents pig serum-induced rat liver fibrosis. Biochem Biophys Res Commun **267**: 290-295.

Humphrey JD, Dufresne ER, Schwartz MA (2014) Mechanotransduction and extracellular matrix homeostasis. Nat Rev Mol Cell Biol **15**: 802-812.

Jennings JM, Dennis DA, Yang CC (2016) Corrosion of the head-neck junction after total hip arthroplasty. J Am Acad Orthop Surg **24**: 349-356.

Kwon YM, Khormaee S, Lincoln MH, Tsai TY, Freiberg AA, Rubash HE (2016) Asymptomatic pseudotumors in patients with taper corrosion of a dual-taper modular femoral stem MARS-MRI and metal ion study. J Bone Joint Surg Am **98**: e93.

Kreplak L (2016) Introduction to atomic force microscopy (AFM) in biology. Curr Protoc Protein Sci **85**: 17.7.1-17.7.21.

Kwon YM, Lombardi AV, Jacobs JJ, Fehring TK, Lewis CG, Cabanela ME (2014) Risk stratification algorithm for management of patients with metal-on-metal hip arthroplasty: consensus statement of the American Association of Hip and Knee Surgeons, the American Academy of Orthopaedic Surgeons, and the Hip Society. J Bone Joint Surg Am **96**: e4. DOI: 10.2106/JBJS.M.00160.

Leonard S, Gannett PM, Rojanasakul Y, Schwegler-Berry D, Castranova V, Vallyathan V, Shi X (1998) Cobalt-mediated generation of reactive oxygen species and its possible mechanism. J Inorg Biochem **70**: 239-244.

Madala SK, Pesce JT, Ramalingam TR, Wilson MS, Minnicozzi S, Cheever AW, Thompson RW, Mentink-Kane MM, Wynn TA (2010) Matrix metalloproteinase 12-deficiency augments extracellular matrix degrading metalloproteinases and attenuates IL-13-dependent fibrosis. J Immunol **184**: 3955-3963.

Madl AK, Liong M, Kovochich M, Finley BL, Paustenbach DJ, Oberdorster G (2015) Toxicology of wear particles of cobalt-chromium alloy metal-on-metal hip implants part I: physicochemical properties in patient and simulator studies. Nanomedicine **11**: 1201-1215.

Matharu GS, Pandit HG, Murray DW, Judge A (2016) Adverse reactions to metal debris occur with all types of hip replacement not just metal-on-metal hips: a retrospective observational study

of 3340 revisions for adverse reactions to metal debris from the National Joint Registry for England, Wales, Northern Ireland and the Isle of Man. BMC Musculoskelet Disord **17**: 495.

Moussavi RS, Kelley CA, Adelstein RS (1993) Phosphorylation of vertebrate monmuscle and smooth-muscle myosin heavy-chains and light-chains. Mol Cell Biochem **128**: 219-227.

Muller ME (1995) The benefits of metal-on-metal total hip replacements. Clin Orthop Relat Res: 54-59.

Myllyharju J, Kivirikko KI (2004) Collagens, modifying enzymes and their mutations in humans, flies and worms. Trends Genet **20**: 33-43.

Natu S, Sidaginamale RP, Gandhi J, Langton DJ, Nargol AVF (2012) Adverse reactions to metal debris: histopathological features of periprosthetic soft tissue reactions seen in association with failed metal on metal hip arthroplasties. J Clin Pathol **65**: 409-418.

Pandit H, Glyn-Jones S, McLardy-Smith P, Gundle R, Whitwell D, Gibbons CL, Ostlere S, Athanasou N, Gill HS, Murray DW (2008) Pseudotumours associated with metal-on-metal hip resurfacings. J Bone Joint Surg Br **90**: 847-851.

Papageorgiou I, Brown C, Schins R, Singh S, Newson R, Davis S, Fisher J, Ingham E, Case CP (2007) The effect of nano- and micron-sized particles of cobalt-chromium alloy on human fibroblasts *in vitro*. Biomaterials **28**: 2946-2958.

Petit A, Mwale F, Zukor DJ, Catelas I, Antoniou J, Huk OL (2004) Effect of cobalt and chromium ions on bcl-2, bax, caspase-3, and caspase-8 expression in human U937 macrophages. Biomaterials **25**: 2013-2018.

Plummer DR, Berger RA, Paprosky WG, Sporer SM, Jacobs JJ, Della Valle CJ (2016) Diagnosis and management of adverse local tissue reactions secondary to corrosion at the head-neck junction in patients with metal on polyethylene bearings. J Arthroplasty **31**: 264-268.

Queally JM, Devitt BM, Butler JS, Malizia AP, Murray D, Doran PP, O'Byrne JM (2009) Cobalt ions induce chemokine secretion in primary human osteoblasts. J Orthop Res **27**: 855-864.

Reddy GK, Enwemeka CS (1996) A simplified method for the analysis of hydroxyproline in biological tissues. Clin Biochem **29**: 225-229.

Rhee S (2009) Fibroblasts in three dimensional matrices: cell migration and matrix remodeling. Exp Mol Med **41**: 858-865.

Rhee S, Grinnell F (2007) Fibroblast mechanics in 3D collagen matrices. Adv Drug Deliv Rev **59**: 1299-1305.

Savarino L, Granchi D, Ciapetti G, Cenni E, Nardi Pantoli A, Rotini R, Veronesi CA, Baldini N, Giunti A (2002) Ion release in patients with metal-on-metal hip bearings in total joint replacement: A comparison with metal-on-polyethylene bearings. J Biomed Mater Res **63**: 467-474.

Shah K M, Wilkinson J M, Gartland A (2015) Cobalt and chromium exposure affects osteoblast function and impairs the mineralization of prosthesis surfaces *in vitro*. J Orthop Res **33**: 1663-1670.

Shulman RM, Zywiel MG, Gandhi R, Davey JR, Salonen DC (2015) Trunnionosis: the latest culprit in adverse reactions to metal debris following hip arthroplasty. Skeletal Radiol **44**: 433-440.

Stroka KM, Aranda-Espinoza H (2011) Endothelial cell substrate stiffness influences neutrophil transmigration *via* myosin light chain kinase-dependent cell contraction. Blood **118**: 1632-1640.

Tang AT, Campbell WB, Nithipatikom K (2012) ROCK1 feedback regulation of the upstream small GTPase RhoA. Cell Signal **24**: 1375-1380.

Tomasek JJ, Gabbiani G, Hinz B, Chaponnier C, Brown RA (2002) Myofibroblasts and mechano-regulation of connective tissue remodelling. Nat Rev Mol Cell Biol **3**: 349-363.

Vicente-Manzanares M, Ma XF, Adelstein RS, Horwitz AR (2009) Non-muscle myosin II takes centre stage in cell adhesion and migration. Nat Rev Mol Cell Biol **10**: 778-790.

Wahl SM, Mccartneyfrancis N, Allen JB, Dougherty EB, Dougherty SF (1990) Macrophage production of TGF-beta and regulation by TGF-beta. Ann N Y Acad Sci **593**: 188-196.

Willert HG, Buchhorn GH, Fayyazi A, Flury R, Windler M, Koster G, Lohmann CH (2005) Metal-on-metal bearings and hypersensitivity in patients with artificial hip joints. A clinical and histomorphological study. J Bone Joint Surg Am **87**: 28-36.

Wynn TA (2007) Common and unique mechanisms regulate fibrosis in various fibroproliferative diseases. J Clin Invest **117**: 524-529.

Zou WG, Yan MD, Xu WJ, Huo HR, Sun LY, Zheng ZC, Liu XY (2001) Cobalt chloride induces PC12 cells apoptosis through reactive oxygen species and accompanied by AP-1 activation. J Neurosci Res **64**: 646-653.

Discussion with Reviewer

Mark Wilkinson: How do these findings contribute to the clinical practice in terms of metals used in joint replacement?

Authors: According to the 15th Annual Report 2018 of National Joint Registry (UK) (Web ref. 1), the number of resurfacing MoM hip replacements continues to decrease, but the MoP bearings are still the most widely used articulation. While revision rate of MoP is the lowest among the implant available, recent reports of MoP failure due to trunnionosis indicate similar adverse response to MoM (Waterson *et al.*, 2018; additional reference), with swelling, pain and an inflammatory mass. These suggest that any joint replacements containing metal component, like cobalt alloy, could lead to similar adverse response. Identifying the mechanism of cobalt-driven adverse response can help in identifying early signs of failure and in developing new safer materials.

Mark Wilkinson: How do the used concentrations of ions compare to those observed clinically in the synovium of patients with CoCr prostheses?
Authors: The choice of ion concentrations was based on previous work on the effect of Co and Cr on different cell lines *in vitro* (Madl *et al.*, 2015). The aim of the current study was to investigate non/cytotoxic concentrations of Co and Cr (Fig. 1). The 200 μM Co^{2+} (≈ 11,786 μg/L) is within the range of Co content detected in synovial fluid from patients with metal-on-metal implants, such as 0 to 24,262 μg/L (Davda *et al.*, 2011) and 11.50-64,550 μg/L (Beraudi *et al.*, 2013, additional reference).

Additional Reference

Beraudi A, Catalani S, Montesi M, Stea S, Sudanese A, Apostoli P, Toni A (2013) Detection of cobalt in synovial fluid from metal-on-metal hip prosthesis: correlation with the ion haematic level. Biomarkers **18**: 699-705.

Waterson HB, Whitehouse MR, Greidanus NV, Garbuz DS, Masri BA, Duncan CP (2018) Revision for adverse local tissue reaction following metal-on-polyethylene total hip arthroplasty is associated with a high risk of early major complications. Bone Joint J **100**: 720-724.

Web Reference

1. http://www.njrcentre.org.uk/njrcentre/Reports,PublicationsandMinutes/Annualreports/tabid/86/Default.aspx [02-10-2018]

Editor's note: The Scientific Editor responsible for this paper was Chris Evans.